Annual and Final Report on the Project **(Grant NO. N00014-96-1-G017)**

Development of Low Loss Multipole RF Filters

September 30, 1999

Q. Y. Ma
Department of Electrical Engineering, Columbia University,
New York, NY 10027
Tel: 212-854-5080, Fax: 212-932-9421

1. Introduction

1.1 Overall

This is a three-year project, started in July 1996 and ended in July 1999. The major objective of the project is to develop low loss multipole RF filters with a band frequency at about 15 MHz. During the project period, we have developed new designs of RF filters with the use of high temperature superconducting (HTS) film [1, 2]. By using HTS device, the low loss and high Q filters were made. With spiral design, the low band frequency at about 15 MHz has been achieved. The highlights made during the project period include

(1) A low insertion loss (-0.7 dB) three-pole filter on a 2-inch HTS wafer

(2) An active switchable tuning method for tunable HTS filter been invented

Related to the research supported by this project there are 2 papers have been published [1, 2], 1 submitted [3], 4 conference papers presented [1, 2, 4, 5] and 2 patent applications submitted [6, 7].

1.2 Report in summary

In the first phase of the project, an interdigital three-pole bandpass filter was designed and fabricated on a 2-inch high temperature superconducting (HTS) film. This interdigital filter,

REPORT DOCUMENTATION PAGE

Form Approved
OMB No. 0704-0188

1. AGENCY USE ONLY (Leave blank)	2. REPORT DATE	3. REPORT TYPE AND DATES COVERED
	08/21/99	Final Report 07/96-07/99

4. TITLE AND SUBTITLE
Development of low loss multipole RF filters

5. FUNDING NUMBERS
N00014-96-1-G017

6. AUTHOR(S)
Q.Y. Ma

7. PERFORMING ORGANIZATION NAME(S) AND ADDRESS(ES)
Columbia University
Department of EE, 1312 Mudd
New York, NY 10027

8. PERFORMING ORGANIZATION REPORT NUMBER
Final (97-99)
including (Annul 99)

9. SPONSORING/MONITORING AGENCY NAME(S) AND ADDRESS(ES)
Dr. Martin Nisenoff, Program officer, Code 6850.10
NRL (Naval Research Laboratory)
4555 Overlook Ave., SW
Washington DC 20375-5326

10. SPONSORING/MONITORING AGENCY REPORT NUMBER

11. SUPPLEMENTARY NOTES

12a. DISTRIBUTION/AVAILABILITY STATEMENT
Approved for public release

12b. DISTRIBUTION CODE

13. ABSTRACT *(Maximum 200 words)*

During contract period, we have completed the technical objectives of this project. The highlights include
(1) Made, for the first time, 3-pole HTS filters in MHz range on 2-inch wafers.
(2) Achieved an insertion loss of -0.7 dB and a return loss of -15 dB.
(3) Invented an active switchable tuning method for turnable HTS filter.

Overall, 2 papers have been published, 3 submitted, 5 conference papers presented and 3 patent applications submitted.

14. SUBJECT TERMS			15. NUMBER OF PAGES
			16. PRICE CODE
17. SECURITY CLASSIFICATION OF REPORT	18. SECURITY CLASSIFICATION OF THIS PAGE	19. SECURITY CLASSIFICATION OF ABSTRACT	20. LIMITATION OF ABSTRACT

NSN 7540-01-280-5500

Standard Form 298 (Rev. 2-89)
Prescribed by ANSI Std. 239-18
298-102

designed by transforming a standard three-pole Chebyshev low-pass filter, consists of 10 interdigital lumped elements: one capacitor and one inductor in each of three resonators and four matching capacitors. The test results demonstrated a three-pole bandpass filter, however, the insertion loss was too high.

In the second phase of the project, the research work was carried out in two directions: improved the old filter structure and developed a new spiral structure filter. The improvements, made to the interdigital capacitor design and fabrication, included adding HTS ground plane, modifying the values of matching capacitors, and optimizing processing recipe. The results showed some improvement on the device performance. However, in this design the matching capacitors are small in capacitance and hard to realize the exact capacitance in fabrication. The characteristics of the filter are very sensitive to those matching capacitors. So we did not succeed to make a satisfactory interdigital filter as we designed. This problem could be avoided by choosing larger matching capacitors, however, the size of the filter will be increased and exceed the available size of the HTS wafer. To solve this problem, a spiral-structure was used in the design of a 24 MHz HTS three-pole bandpass filter. The filter consists of three self-resonant spirals and one input and one output coupling loops. Three different configurations of input/output coupling loops were used in order to optimize the filter performance: big-loop, small-loop-near, and small-loop-far. The best result of these three configurations of coupling was obtained from small-loop-far coupling which gave the three-pole center frequency of 24 MHz, an insertion loss of -2 dB, a return loss of -5 dB, and a stopband of < -40 dB. The progress of the project was made with using the spiral-structured filter design in decreasing insertion loss, increasing return loss and increasing stability and repeatability in fabrication.

In the third phase of the project, the research work was carried out in improvement of the spiral-structured filter and in design of a frequency switchable filter. First, some modifications were made to the spiral-structured filter design and fabrications. We made much progress of the project with the new spiral filter design in decreasing insertion loss, increasing return loss and increasing stability and repeatability in fabrication. The best result obtained gave the three-pole center frequency of 18 MHz, with an insertion of -0.7 dB, and a return of -15 dB. Second, for the switchable filter, we explored a frequency switch circuit of the HTS RF device using active electronic control (current or voltage), in which a resonator was magnetically coupled with an

HTS switch circuit, a resonator by itself. When the control current (or voltage) applied to the switch circuit was zero (off), the two resonators were in superconducting state and coupled with each other forming a resonator with frequency f_1. By converting one resonator into non-superconducting state using controlling current (or voltage), we were able to change the resonant frequency into the resonant frequency of the resonator remained in superconducting state, f_2. A frequency shift of a switchable resonator from 95.7 MHz to 101 MHz was obtained with a control voltage.

1.3 Conclusion

Multipole RF filters with low insertion loss, low band frequency (MHz range), and small size can be achieved by using spiral design on HTS film. The band frequency of the filter can be switched from one to another by using another HTS device, which is actively tuned by a control current or voltage.

2. Design and fabrication

2.1 first approach--interdigital design

The bandpass filter was transformed from a standard 3-pole Chebyshev low-pass filter. The target specifications are shown as below.

Central Frequency f_0	15 MHz
Band width (BW)	15 kHz (0.1% f_0)
Insertion Loss (S12)	< 0.3 dB
Return Loss (S11)	< -20 dB
Stop Band at 4 times BW	< -40 dB

The interdigital three-pole HTS filter design and its equivalent circuit are shown in Fig. 1 and Fig. 2. Simulations were performed with HP EESof, a simulation suite of microwave communication circuit, as shown in Fig. 3.

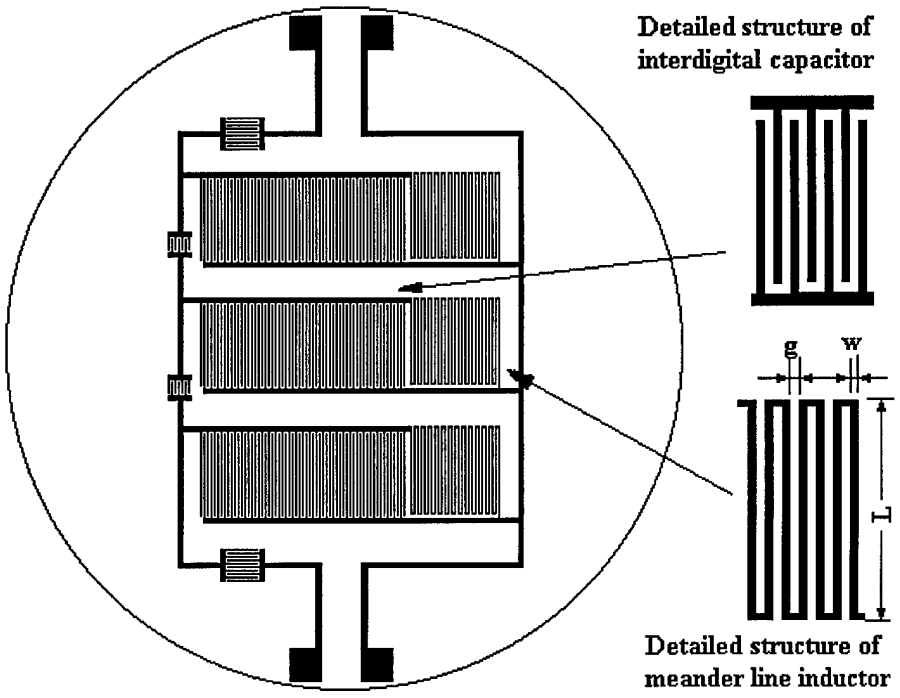

Fig. 1. The structure of a three-pole HTS filter designed on a 2-inch wafer. The circuit is realized by coplanar microstrip line. The capacitors and inductors

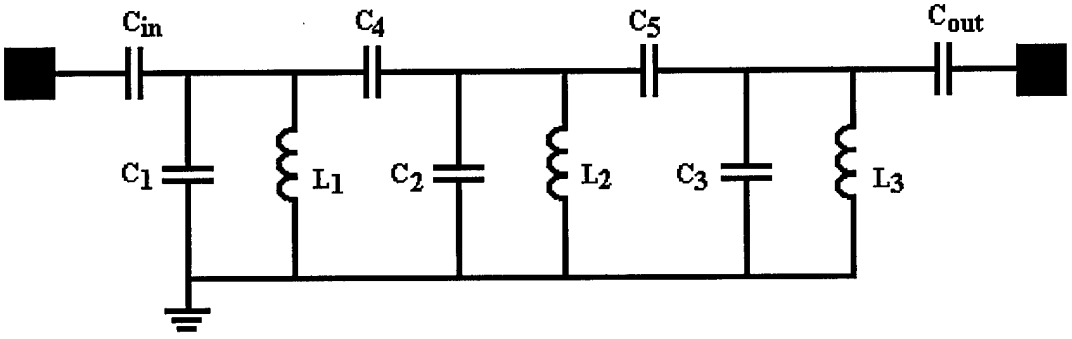

Fig. 2. Equivalent circuit of the three-pole interdigital filter

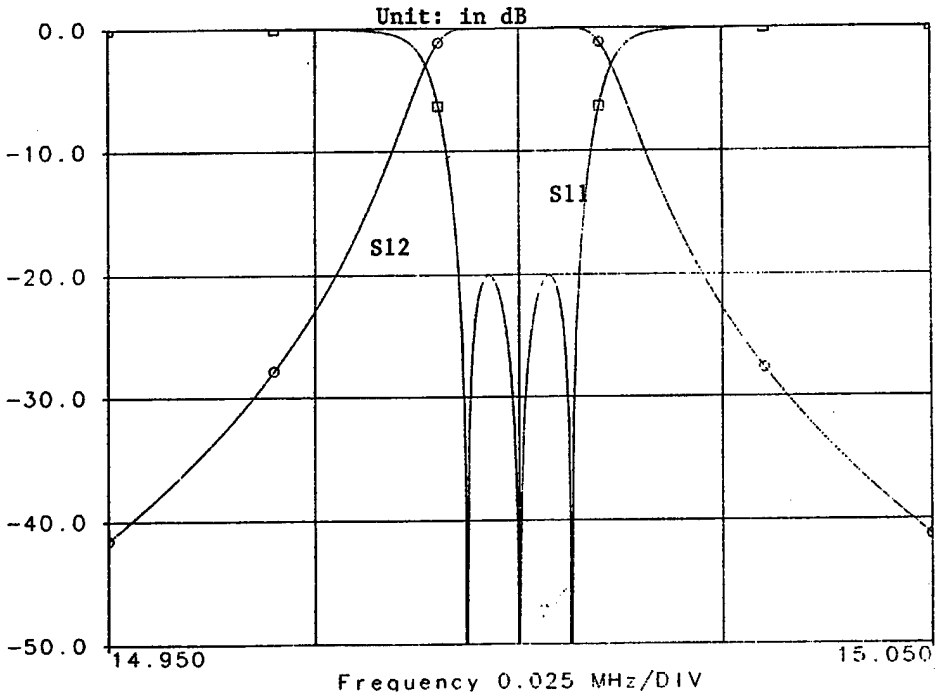

Fig. 3. Circuit simulation result with HP EESof.

To implement such a circuit on HTS thin film, we have chosen corresponding microstrip line structure. Since the inductor model in EESof library requires a gold bridge to connect the center lead to the outside one, which causes too much additional loss, we have used the Meander Line Inductor instead to maintain the coplanar structure. The use of meander line inductors

increased the total area slightly but minimized the loss due to wire banding. The final layout fitted well in a 2-inch wafer.

A model for the meander line structure was built to implement the filter. The inductance is calculated with the following formula:

$$L = Ls + M \qquad (\mu H) \tag{1}$$

where Ls is the self-inductance of all lines (total number of n) and M is the mutual inductance between lines with both units in μH [8].

$$Ls = 2\times 10^{-4} n\times(l+g)\times \log(\frac{l+g}{w+t}+1.193+0.\qquad \frac{w+t}{l+g}), \tag{2}$$

$$M = 2\sum_{i=1}^{n-1}\sum_{j=i+1}^{n}[(-1)^{i-j}\frac{\mu}{4\pi}\times 10^3\times l\times(2\sqrt{a^2}-2\sqrt{1+a^2}+\log\frac{\sqrt{1+a^2}+1}{\sqrt{1+a^2}-1})], \tag{3}$$

$$\text{where } a=(i-j)\frac{g}{l}, \tag{4}$$

t is the thickness of the HTS film, w, g and l are shown in Fig. 1 with the units in μm.

2.2 Second approach--distorted spiral design

In the distorted spiral filter design, three self-resonant spiral resonators are place on a 2-inch HTS wafer, as shown in Fig. 4. Each spiral contained 20 turns with homogeneous separation between adjacent turns. These three spirals were arranged in parallel to each other and mutually coupled. Two coupling loops were used to input and output the signal. Three different configurations of pick-up loops were designed and fabricated to optimize the performance. The three different kinds of coupling include (a) big-loop configuration, (b) small-loop-near configuration, and (c) small-loop-far configuration, as shown in Fig. 5. In the big-loop configuration, half of the three resonators are covered on one side by a large input loop and the other half on the other side by another large output loop. In the small-loop-near configuration, the signal is coupled in and out of the filter through the middle resonator by two small coupling

loops. In the small-loop-far configuration, the signal is coupled in the filter through the resonator on one side by a small coupling loop and out of the filter through the resonator on the other side by another small coupling loop, as shown in Fig. 5. The coupling loops were made of fine copper wires and connected to coaxial cables.

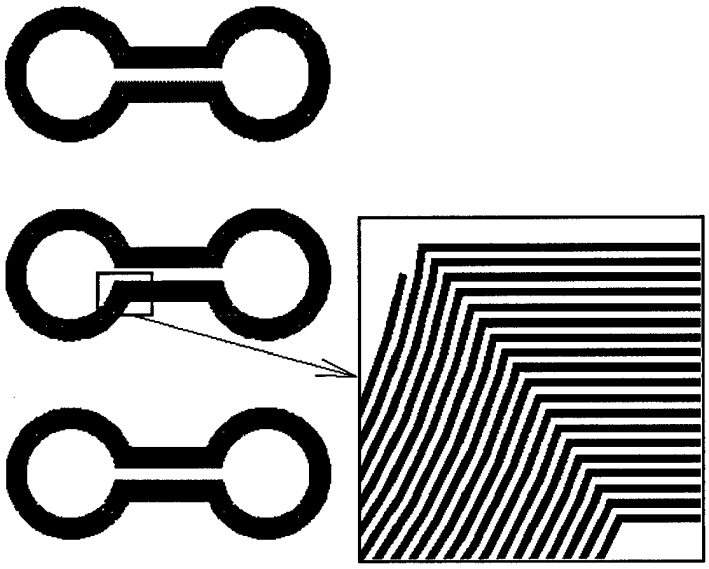

Fig. 4. Three self-resonant spirals are placed together to form a three-pole HTS filter

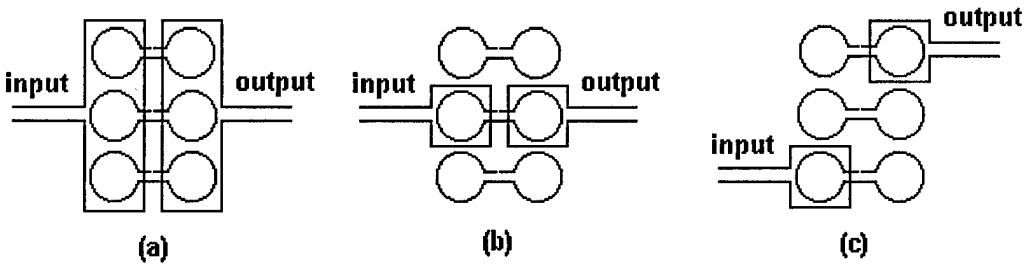

Fig. 5. Three coupling configurations of the three-pole HTS filter with two copper loops: (a) big-loop, (b) small-loop-near, and (c) small-loop-far

2.3 Third approach--elliptic spiral design

In the elliptic spiral design of the three-pole filter, there are three separated, however, closely located resonators and two pick-up loops which are placed on the top of two resonators, as shown in Fig. 6 (a). The three resonators, identical in shape and size with each other, were

made of HTS thin film, patterned and fabricated on a two-inch wafer with an HTS thin film (300 nm YBCO on LAO substrate with 0.508 mm of thickness), as shown in Fig. 6 (b). The resonator is a self-resonant elliptic spiral, of which the shape is a combination of two half circle on the two ends of a rectangular. The spiral contains 25 turns with homogeneous separation between adjacent turns, as shown in Fig. 6 (c). The two pick-up loops are made of copper wire with the same shape and size of the HTS resonators.

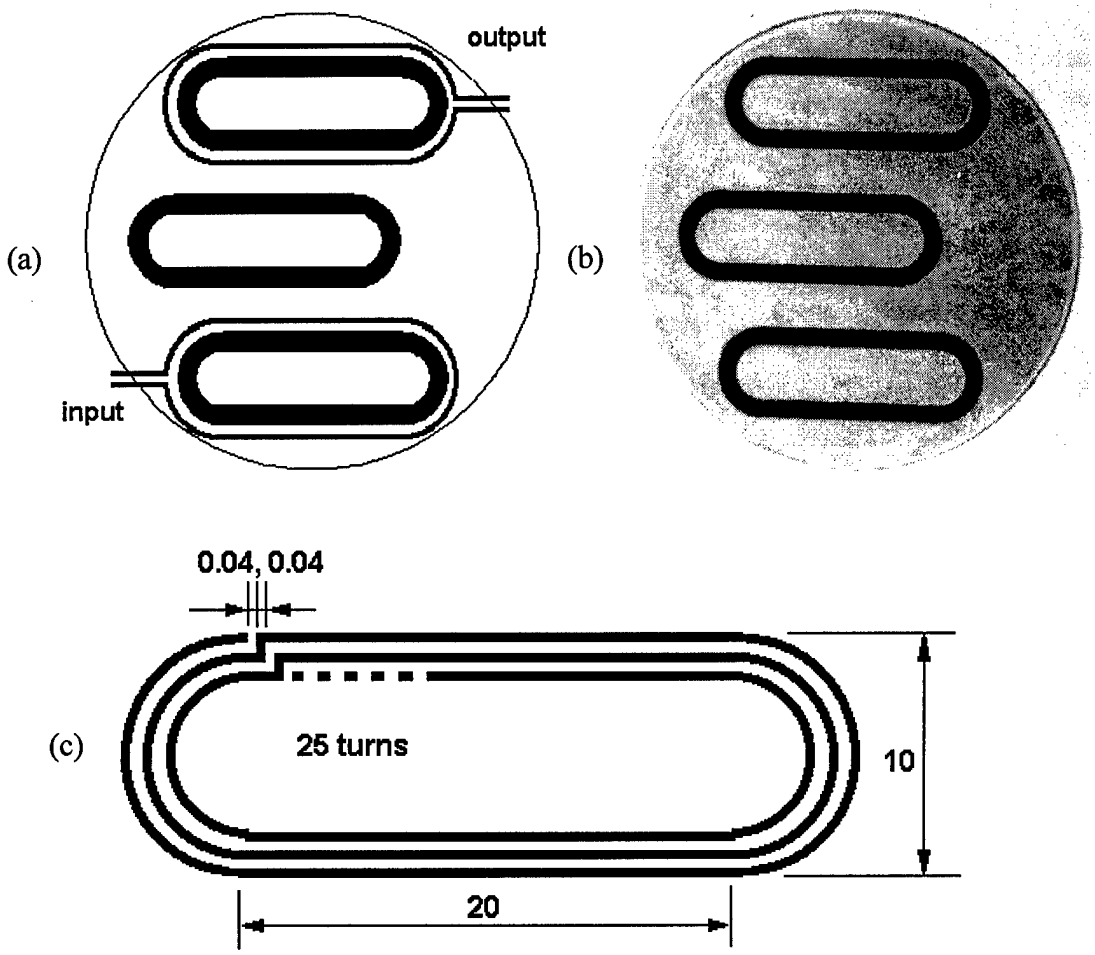

Fig. 6. A elliptic spiral three-pole HTS filter made of three HTS resonators and two copper coupling loops (a). The three HTS resonators were fabricated on a 2-inch LAO substrate (b). The detailed structure of one of the three self-resonant spirals used in the three-pole HTS filter is shown in (c).

The self-resonant elliptic spiral resonator was simulated using an equivalent circuit with lumped elements as shown in Fig. 7. V represents source. R_1=50 Ohm, the input resistance. R_2 is the loss resistance of the spiral. C_2 is the effective inter-turn capacitance. L_1 is the inductance of the pick up loop. L_2 is the effective inductance of the spiral. The inductance can be calculated by

$$L_2 = 0.03937\frac{a^2n^2}{8a+11w}$$
$$L_1 = \frac{1}{n^2}L_2 \qquad (5)$$

where the inductance is in nanohenry, a is the effective radius of a circular spiral in micron, w the width of the spiral, and n the number of turns of the spiral, as shown in Fig 7. The effective radius of our noncircular spiral was calculated by

$$a = \sqrt{\frac{\text{area of a spiral}}{\pi}}. \qquad (6)$$

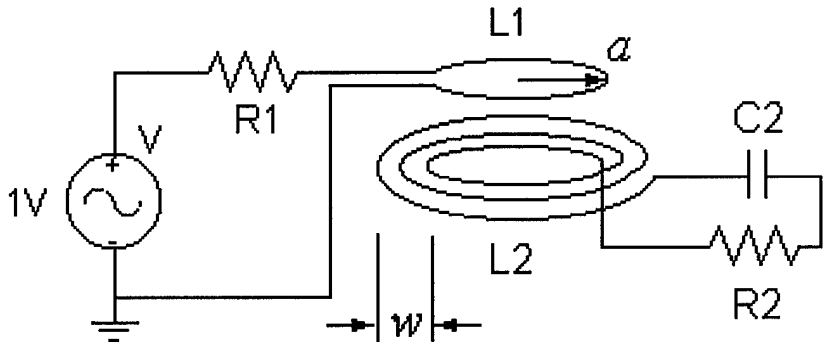

Fig. 7. Model of the self-resonant spiral resonator

The coupling between L_1 and L_2 was described by a mutual inductance, M_{12}. As an approximation, M_{12} can be calculated as following. Assume L_1 is placed on the top of L_2, the total inductance is

$$L_t=(n+1)^2L1 \qquad (7)$$
$$=L_1+L_2+2M_{12}$$
$$=n^2L_1+L_1+2M_{12} \qquad (8)$$

From (7) and (8), one can have $M_{12}=nL_1$.

If k ($0<k<1$) is used to stand for the coupling coefficient between L_1 and L_2 when they are not placed on top of each other, we have

$$M_{12} = knL_1, \tag{9}$$

The circuit can be analysed by

$$\begin{aligned} R_1 I_1 + j\omega L_1 I_1 + j\omega M_{12} I_2 &= V \\ j\omega M_{12} I_1 + j\omega L_2 I_2 + \frac{1}{j\omega C_2} I_2 + R_2 I_2 &= 0 \end{aligned} \tag{10}$$

where $\omega=2\pi f$ is angular frequency and $j=\sqrt{-1}$. Fig. 8 shows the simulated S_{11} as a function of frequncy and coupling coefficient k. One peak was found at k=0.042.

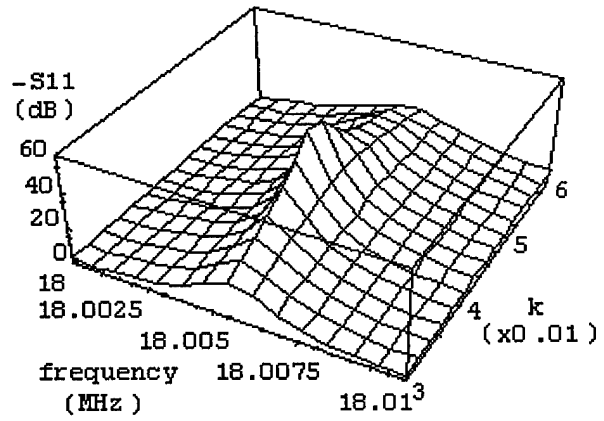

Fig. 8. The reflection of a self-resonant spiral resonator as a function of frequency and coupling coefficient, k, between the pick-up loop and the resonator.

A circuit model of the three-pole filter that is shown in Fig. 9 was simulated simularly to the self-resonant spiral resonator. The simulated results of reflection and insertion are shown in Fig. 10 and Fig. 11.

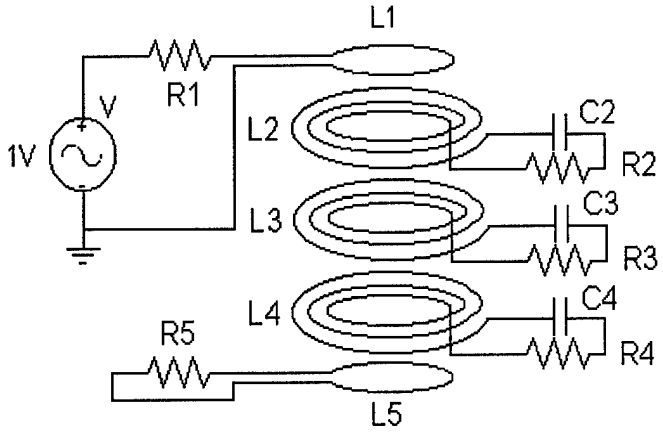

Fig. 9. A model of three-pole spiral filter.

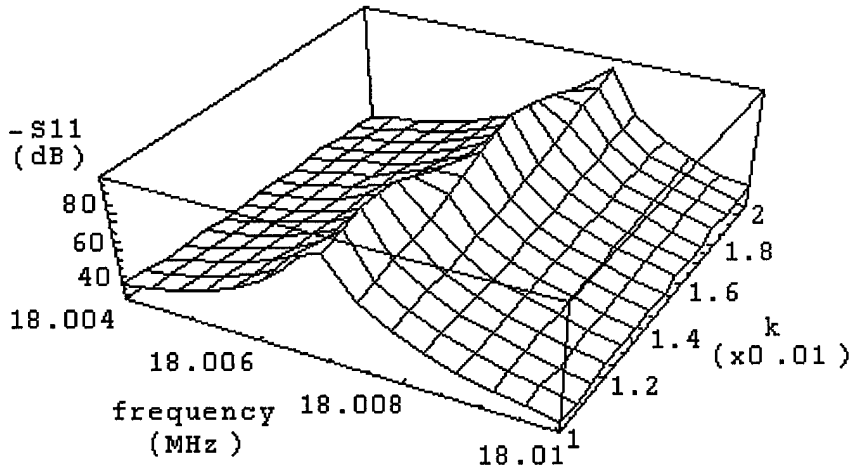

Fig. 10. The reflection of a three-pole spiral filter as a function of frequency and coupling coefficient, *k*, between the coils and pick-up loops.

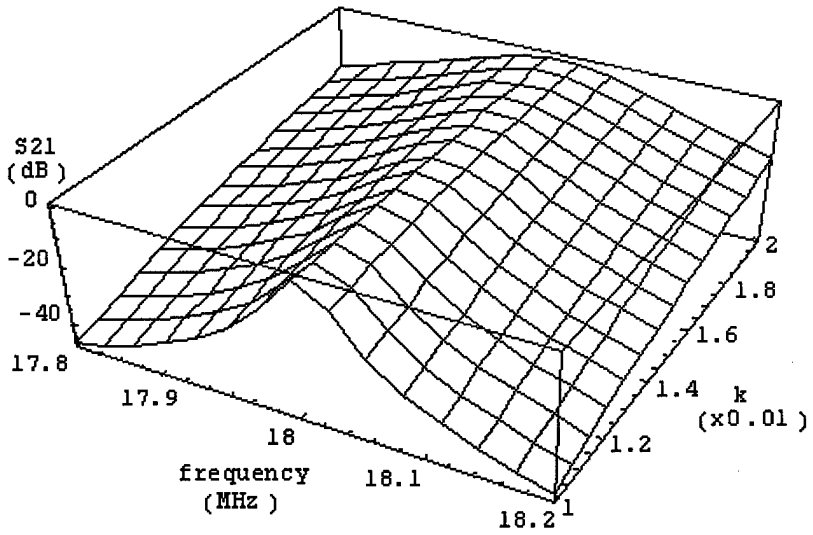

Fig. 11. The insertion of a three-pole spiral filter as a function of frequency and matching coefficient, k, between the coils and pick-up loops.

3. Fabrication, Testing and Analysis

3.1 interdigital three-pole HTS filter

Two filters and several individual capacitors and inductors were fabricated on three two-inch wafers (200 nm YBCO on 20 mil LAO substrate). After that, 50-nm silver and 150-nm gold was deposit as contact pads.

Two filters, labeled as filter1 and filter2, were tested in Naval Research Laboratory at a standard microwave test bed. The temperature in the system could be adjusted from room temperature down to 10K. An Indium/gold plate was used as grounding plane. All filters were tested at different temperature (13K, 30K and 50 K) and different input power level. The result is shown in Table1. After testing, condensation was found on filter2 during warm-up process, which degraded the superconductor. Fig. 12 is S-parameter response of filter1.

Table 1. Test result of filters

Filter	Tc (K)	f_0 (MHz)	BW(kHz)	I. L. (dB)	Pass Band Ripple (dB)
filter1	60-70	18.25	300	-20	10
filter2	50-60	17.7	60	-15.4	2
design	-	15	15	0.3	0.3

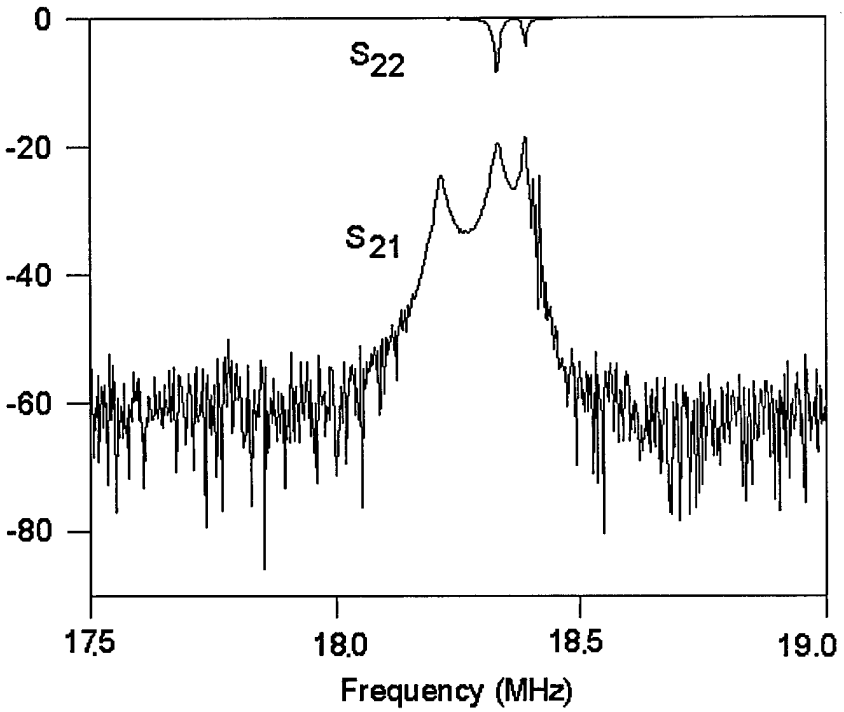

Fig. 12. Response of the filter made in May 1997

It could be seen in Table 1 that the central frequency is off about 20%, and the bandwidth is much larger than our design. Insertion loss and pass band ripple is higher than expected. Besides, the sample is power sensitive. The response is completely suppressed at normal power levels (0 dBm or 1mw) though this is a common phenomenon for HTS microwave devices. The power was set to -20 dBm for all measurements.

Several interdigital capacitors and meander line inductors were also tested in order to get more precise model and improve our design.

The capacitor and inductor in each resonator determined the central frequency. The test result of interdigital capacitor shows that the capacitance derivation is within 2% as designed, which is fairly good. But the result is not the same for meander line structures. It was necessary to test more inductors and to improve the model.

The bandwidth, insertion loss, and pass band ripple are related to resonator structure used in the filter, especially, to the coupling capacitors between each resonator.

The coupling capacitor is several orders smaller than the resonance capacitor (about 0.2 pF compared to 200 pF). Taking account of the parasitic capacitance of the interconnect microstrip line and inaccuracy due to fabrication, the derivation could be the same order as the capacitor itself. These led to a wide pass band, a large insertion loss, and pass band ripple. After changing the coupling capacitors by an offset with the same order, we got the simulation result similar to our experiment.

To improve the interdigital design, first we verified the individual elements, capacitor and inductor. Two testing structures were made and sent to NRL for testing in November 1997. The result, as shown in Fig. 13, agrees with our simulation. The phases of the inductor and capacitor are 90 degree and -90 degree at 15 MHz, respectively, which indicated that our model used in individual element design is satisfactory.

Two more devices were made and tested at Columbia afterwards and the results (Fig. 14) are summarized as below:

Table2. Summary of continuing work on old design

Device	BW	I.L.	R.L.	Temp.	Power	comments
1	8 MHz	-2 dB	-12 dB	26 k	-10 dBm	BW wide
2	8.4 MHz	-2 dB	-10 dB	26 k	-10 dBm	BW wide

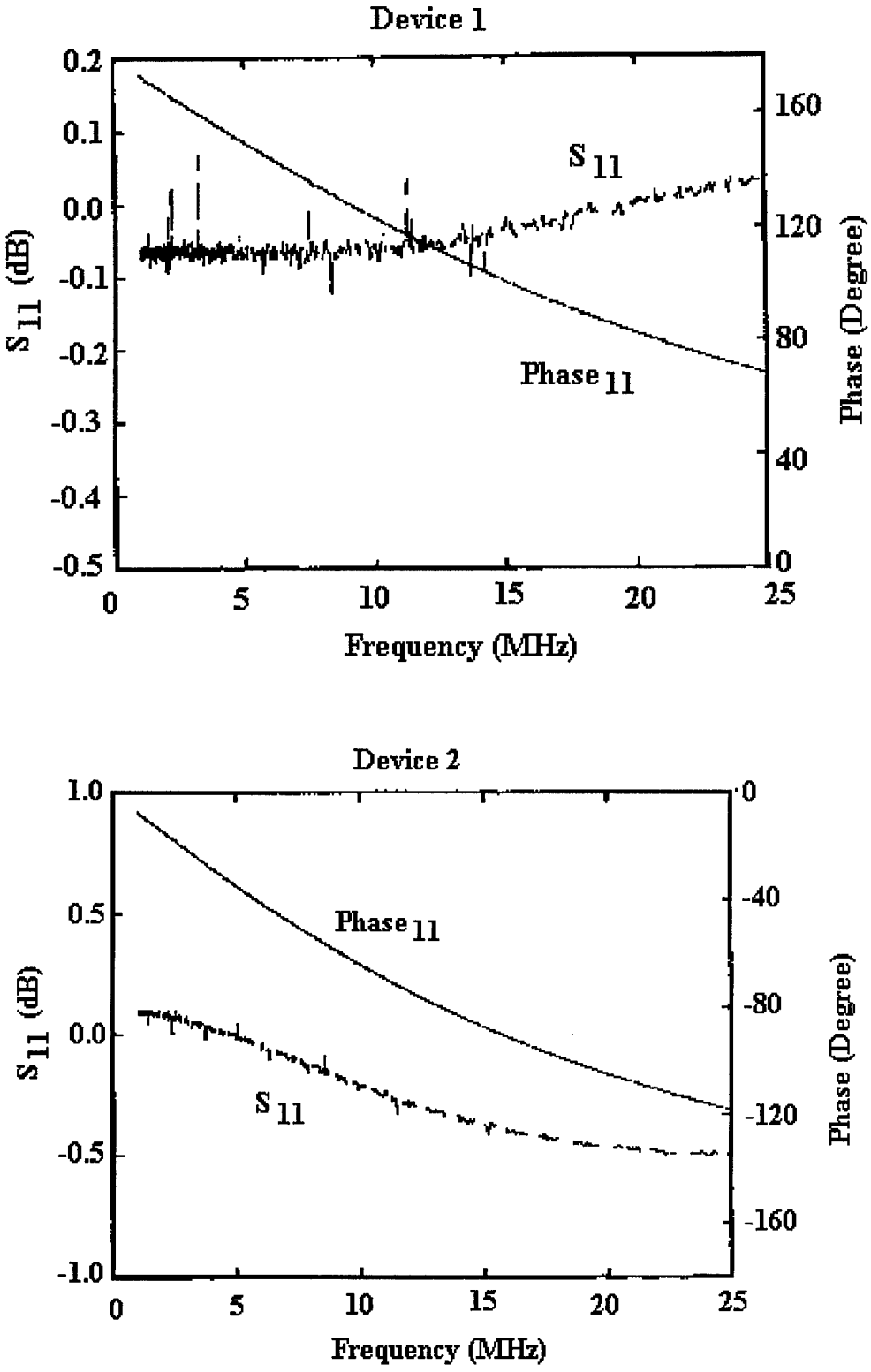

Fig.13. Testing results of an inductor (Device 1) and a capacitor (Device 2) made with YBCO film

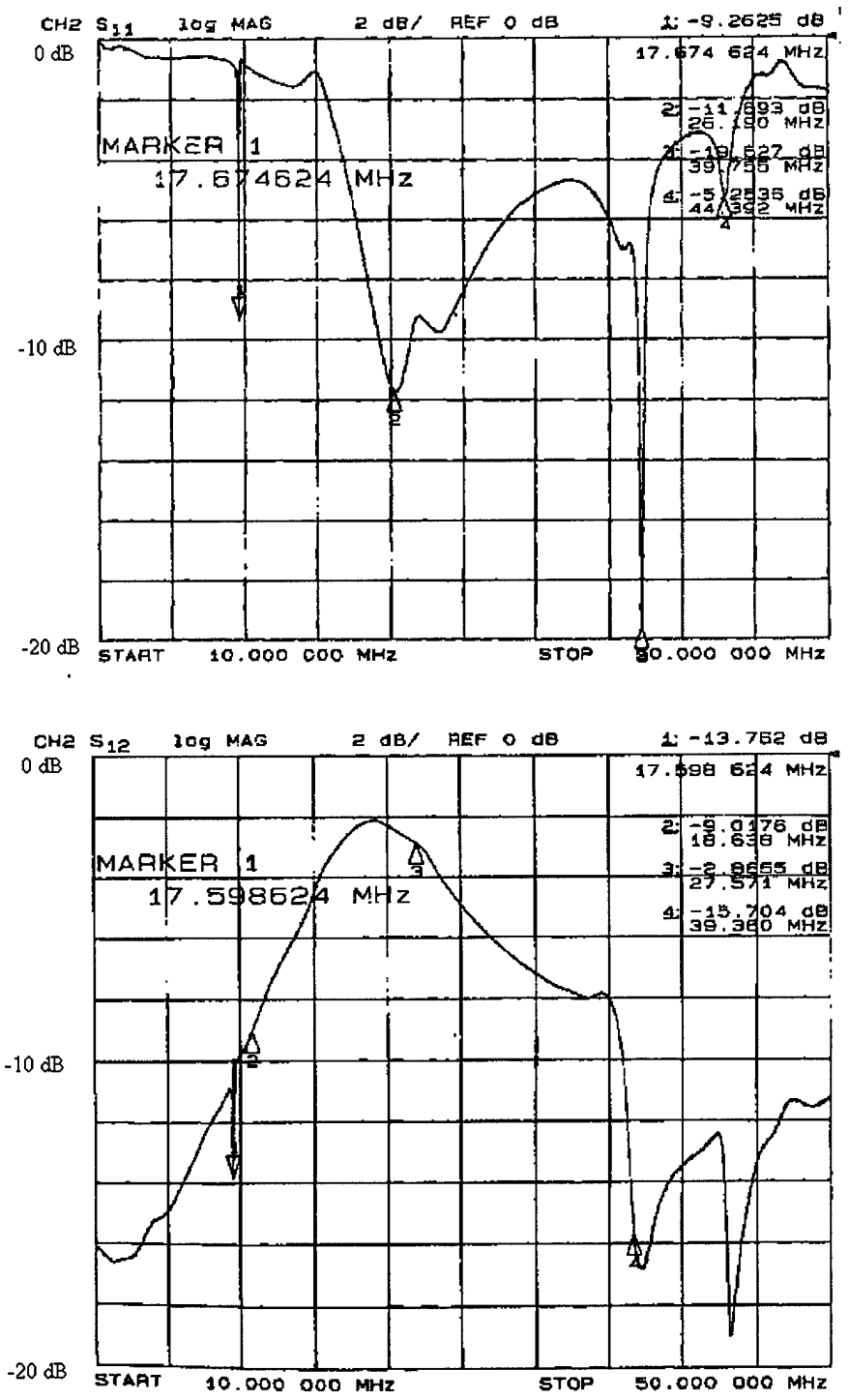

Fig. 14. Response of filter made in May 1998 shows lower insertion loss and high return loss, but with a widened bandwidth

Compared with the results obtained in the first phase of the project, the insertion loss and return loss were improved from -20 dB to -2 dB for insertion loss and from -1 dB to -10 dB for return loss. But the bandwidth of the filter response was widened. The tested results of individual elements were in good accordance with our simulation. We believe that the deference in the performance of the filter from the design is due to the mismatching between resonators and the mismatching between the filter and the testing equipment. The frequency of this design can not be changed easily for the following reasons. To achieve narrow bandwidth and low insertion loss, our design were made from large capacitors (~200 pF) for resonant and very small capacitors (~0.2 pF) for matching. The characteristics of the filter are very sensitive to the values of matching capacitors. Therefore, the distributed parasitic capacitance or inductance and the variation of the values of the elements from fabrication are big enough to change the characteristics of the filter significantly. Based on the analysis we shifted our focus to the new structure in the later stage of the project discussed below.

3.2 Distorted spiral three-pole HTS filter

Three 3-pole-filters were tested in liquid Nitrogen at 77K with three different coupling loops, as shown in Fig. 5 (a), (b), and (c). Return loss (S_{11}) and insertion loss (S_{12}) were measured with a HP-8712B RF Network Analyzer. Three peaks were found in S_{11} and S_{12} for all three filters, as shown in Fig 15, 16, and 17. The three peaks measured with small-loop-far (c) were less separated.

(a) Big-loop (#S1, Fig. 15)

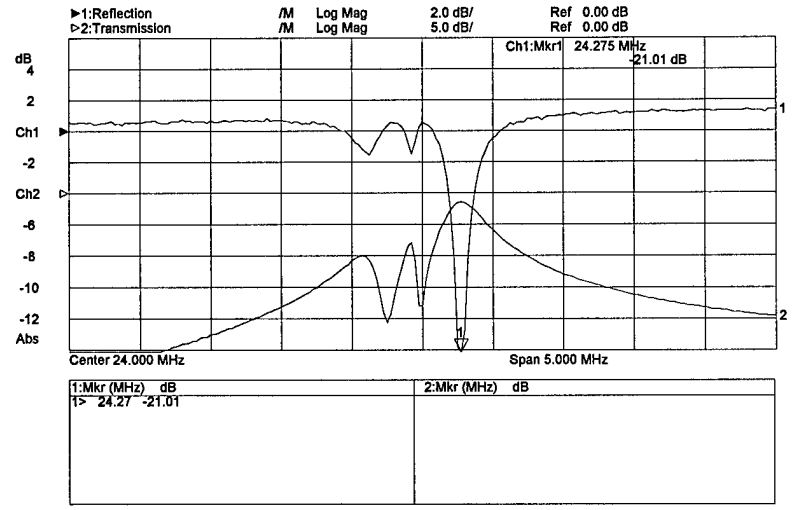

Fig.15. Return loss (S_{11}) and insertion loss (S_{12}) measured with big-loop (#S1)

(b) Small-loop-near (#S2, Fig. 16)

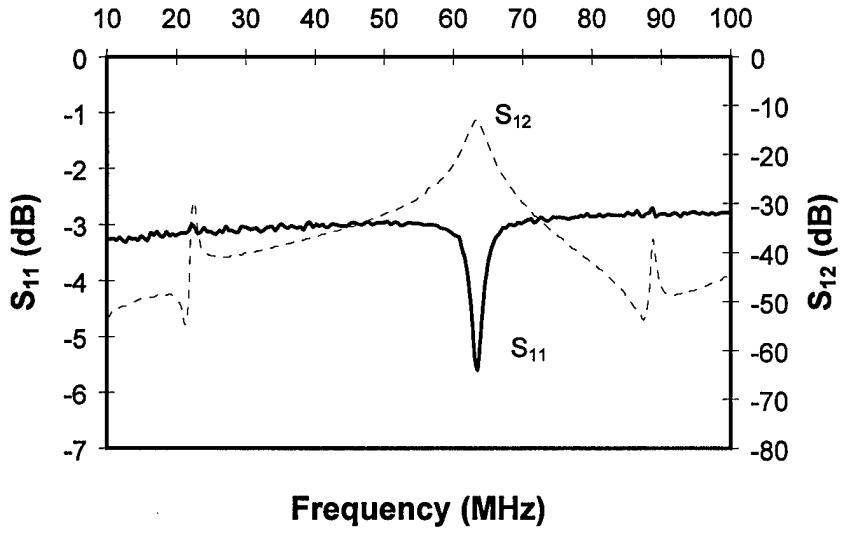

Fig. 16. Return loss (S_{11}) and insertion loss (S_{12}) measured with small-loop-near (#S2)

(c) Small-loop-far (#S3, Fig. 17)

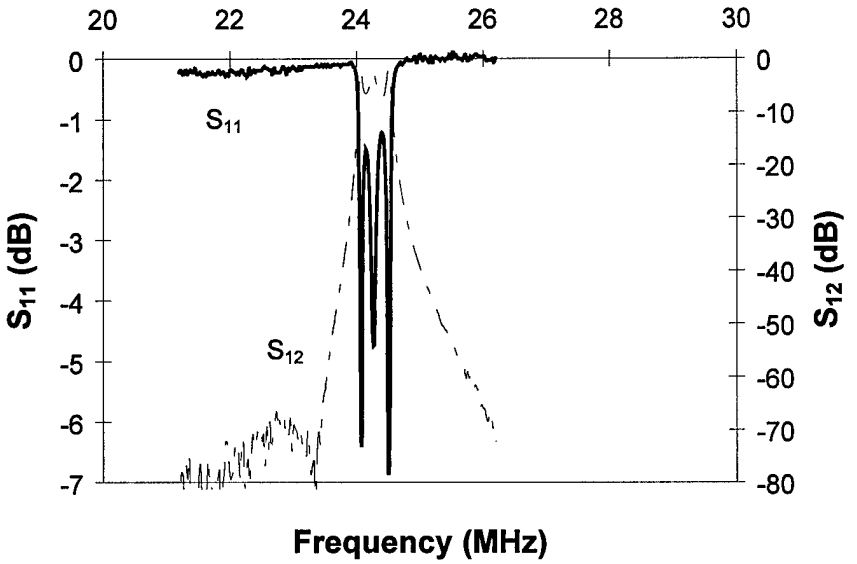

Fig. 17 Return loss (S_{11}) and insertion loss (S_{12}) measured with small-loop-far (#S3)

The bandwidth was about 0.43MHz. The maximal insertion loss between 24.07 and 24.50 MHz is -6.91 dB. At lower (<23.77 MHz) or higher (>25.03 MHz) frequency the insertion loss were lower than -40 dB. Based on these results a patent application was filed for the new design.

The new designed 3-pole filters with two small coupling loops (far) had three poles at about 24 MHz and distributed in about 0.5MHz. The insertion loss was about -2dB and return loss is about -5dB. Even though this design was not satisfactory, it was closer to our aims.

3.3 Elliptic spiral three-pole HTS filter

A single spiral was tested at 77 K as a resonator with a copper coupling loop. The reflection of this spiral resonator is shown in Fig. 18. The resonant frequency is 17.855 MHz and unloaded Q-value is over 13,000. Based on this resonator design, a three-pole filter was designed, fabricated, and tested. The result obtained gave the three-pole center frequency of 18 MHz, with an insertion of -0.7 dB, and a return of -15 dB as shown in Fig. 19 [3].

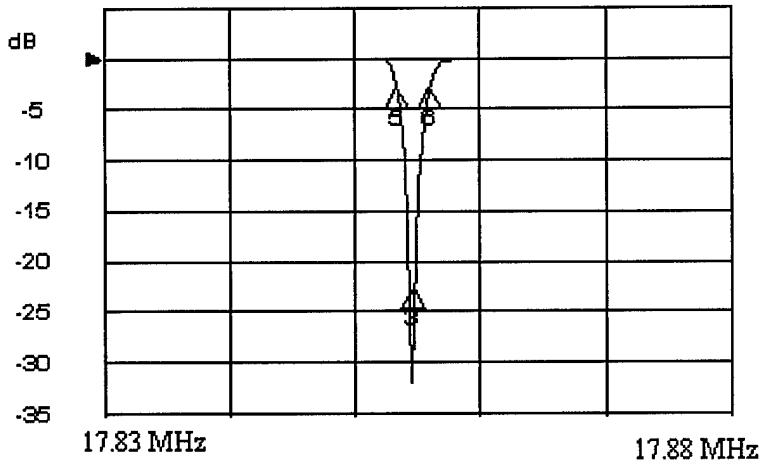

Fig. 18. Measurement of the reflection of a 25-turn spiral resonator at 18 MHz.

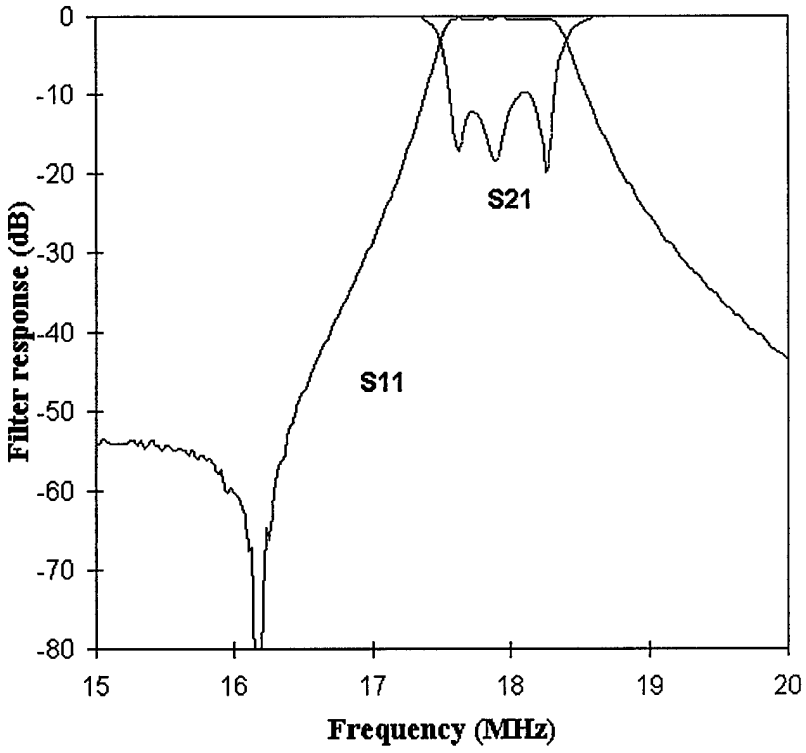

Fig. 19. Return loss (S_{11}) and insertion loss (S_{12}) of an HTS three-port filter.

In the third phase, the work has been focused on two topics: improving the spiral filter and design switchable filter. Some modifications were made to the spiral design and fabrications. The project has made much progress with the new spiral filter design in decreasing insertion loss,

increasing return loss and increasing stability and repeatability in fabrication. The best result obtained gave the three-pole center frequency of 18 MHz, with an insertion of -0.7 dB, and a return of -15 dB.

Based on the design and the results of the second phase of the project, we have made a new design, or an elliptic spiral design, which has smaller bandwidth, lower insertion loss and higher return loss, and higher Q.

4 Tunable switching and future work

4.1 switchable circuit

To approach active frequency tuning device, the previous proposed design was using a ferroelectric-HTS hybrid structure. However, our experiment showed that the presence of ferroelectric material decreased the Q value of HTS device so the resonant peak disappeared. We modified our approach and explored a frequency switch circuit of the HTS RF device using active electronic control (current or voltage), in which a resonator (Part A in Fig. 20) was magnetically coupled with an HTS switch circuit (Part B in Fig. 20, also a resonator of itself). Part A and Part B were fabricated on two separated films. The electrical control signal was applied through two gold wires bonded to the two ends of the switch circuit (Part B). The wire bonding process is commonly used to make connections in micro processing. When the switch K was off, the two resonators were in superconducting state and coupled with each other, and formed a resonator with frequency f_1. By converting Part B of the device into non-superconducting state using controlling current or voltage (K was on), we were able to change the resonant frequency into the resonant frequency of Part A, f_2. A frequency shift of a tunable resonator from 95.7 MHz to 101 MHz with a control voltage was obtained, as shown in Fig. 21. This result is very encouraging since it shows an innovative method of tuning for HTS devices.

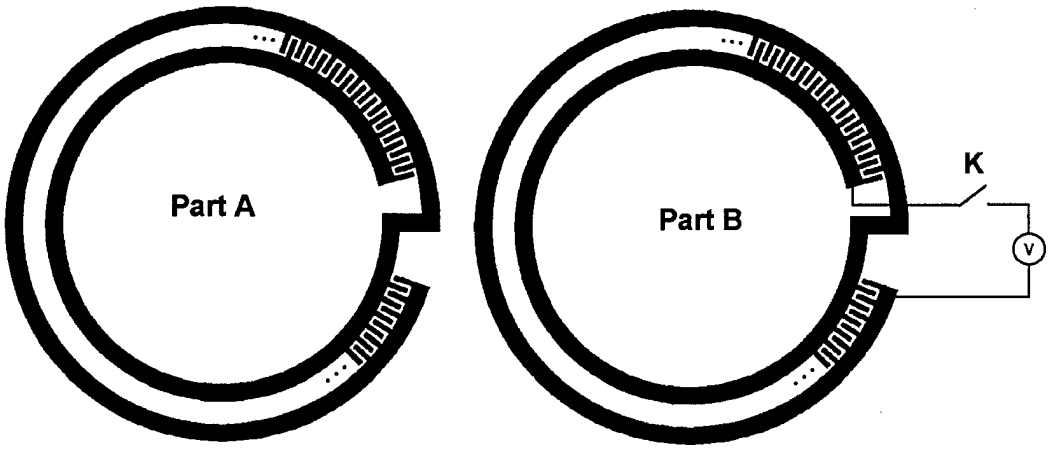

Fig. 20. Layout of an HTS tunable resonator consist of a HTS resonator (Part A) and an HTS switch circuit (Part B). The resonant frequency can be changed with turning on or off the voltage control signal.

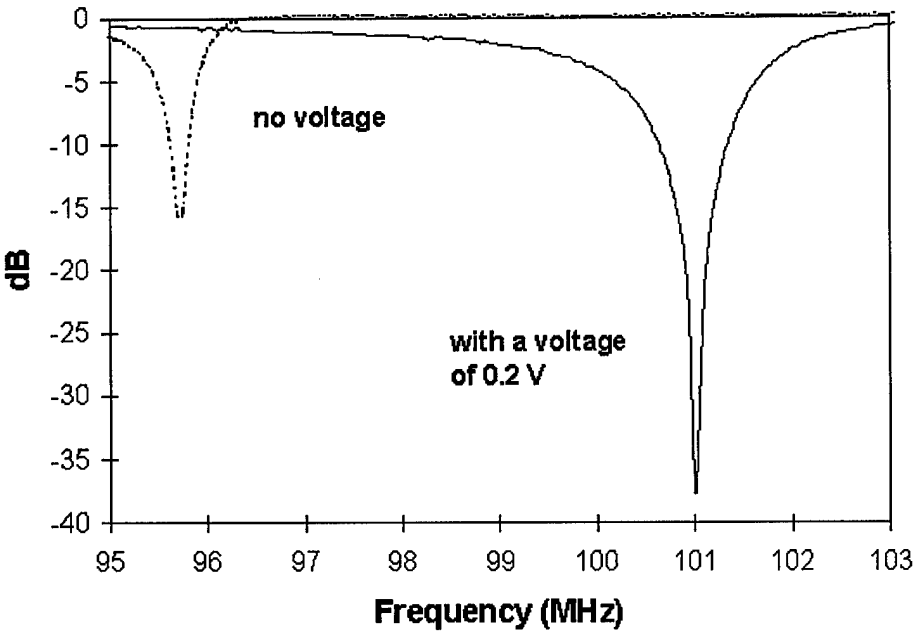

Fig. 21. Response of a tunable resonator with an active voltage control.

The bandwidth is about 0.43MHz. The maximal insertion loss between 24.07 and 24.50 MHz is -6.91 dB. At lower (<23.77 MHz) or higher (>25.03 MHz) frequency the insertion loss are lower than -40 dB. Based on these results a patent application was filed for the new design.

The depth of the notch changed from -15 dB to -35 dB, which was due to the change of matching. In this design the matching between the pick up loop and the filter could not be changed during one test. New designs are proposed in Section 4.2, of which the matching problem will be addressed.

4.2 Future work and active frequency-tuning mechanism----capacitor-tuning

In order to get continuous frequency tuning ability, a new electrical/mechanical approach, capacitor-tuning, is designed for future research. The resonator is formed of an HTS inductor and a variable capacitor that consists of two separated parts: movable and fixed. The layout of the variable capacitor is shown in Fig. 22. The movable part was mounted on a piezoelectric bender or tube actuator so its position can be changed with changing the control voltage of the bender or tube actuator. Two examples of the piezoelectric bender or tube actuator are described in Appendix II. The frequency of the resonator depends on the value of the inductor and the

capacitor. The value of the capacitor can be changed with changing the relative position of the movable part to the fixed part. Fig 23. (A) and (B) shows two possible ways to use piezoelectric bender or tube actuator to change the position of the movable part of the variable capacitor in the tunable resonator design. Fig. 24 shows another design of the variable capacitor in the tunable resonator, which will provide higher sensitivity of the capacitance to the position and therefore higher sensitivity in tuning frequency.

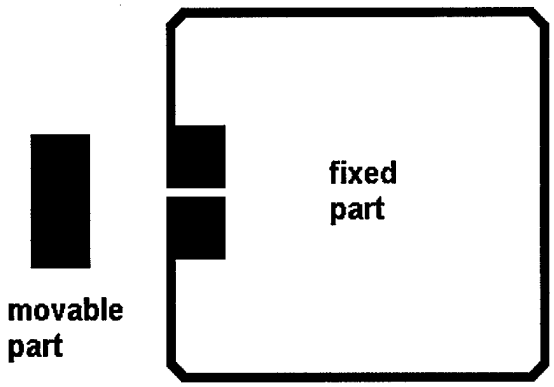

Fig. 22. A new electrical/mechanical approach to tunable filter using HTS film and piezoelectric material

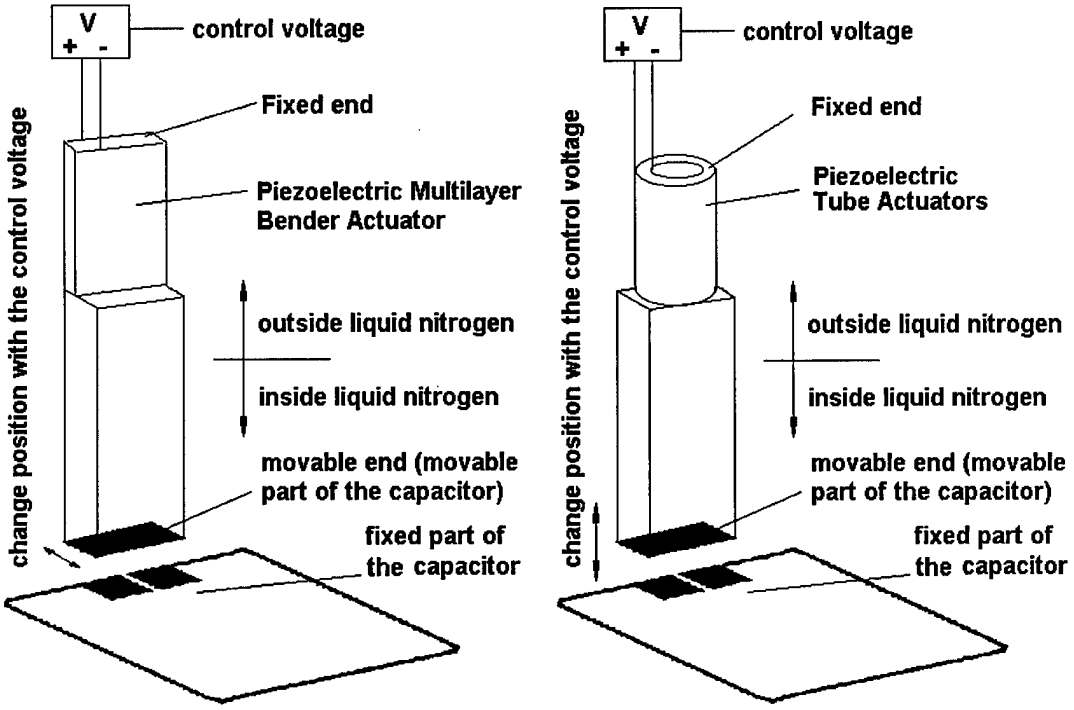

Fig. 23. Two possible ways to use piezoelectric bender or tube actuator to change the position of the movable part of the variable capacitor in the tunable resonator design.

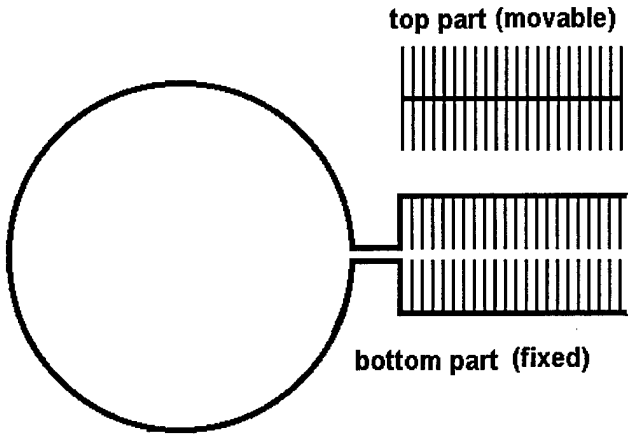

Fig. 24. The possible layout of HTS film for a new electrical/mechanical approach to tunable resonator that will provide higher sensitivity.

Using three tunable resonators as described above to form a three-pole filter as described in elliptic spiral filter design, where the spiral coils were replaced by three capacitor-tuning resonators, a three-pole tunable HTS filter was designed. The fixed parts of the three capacitor-tuning resonator and two pick-up loops were fabricated on one substrate with HTS film. The layout is shown in Fig. 25. The movable parts of the filter were three movable parts of three resonators as shown in Fig. 23. Three piezoelectrical actuators (benders or tubes) were used to tune the frequency of each resonator, therefore to tune the bandwidth and center frequency of the filter. Demonstrated in Fig. 26, a tunable capacitor can be used to change matching.

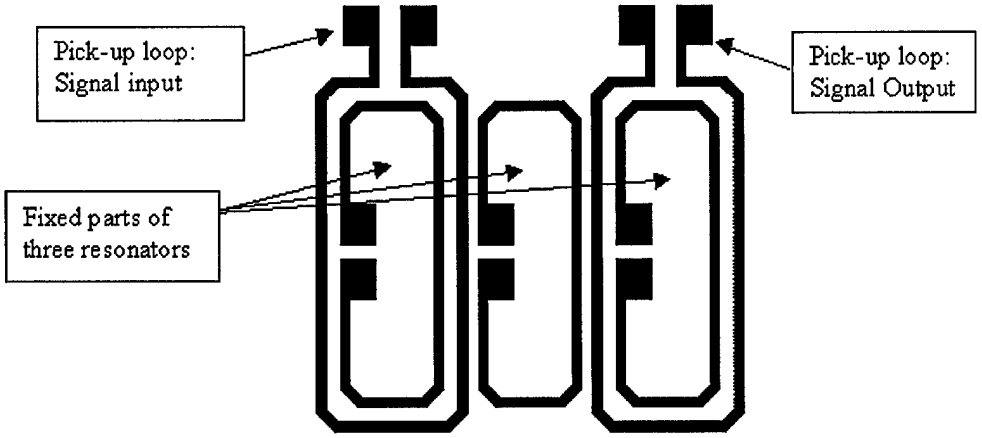

Fig. 25. Layout of the fixed part of a three-pole active tunable HTS filter, which consists of the fixed parts of three capacitor-tuning resonator and two pick-up loops which were fabricated on one substrate with HTS film.

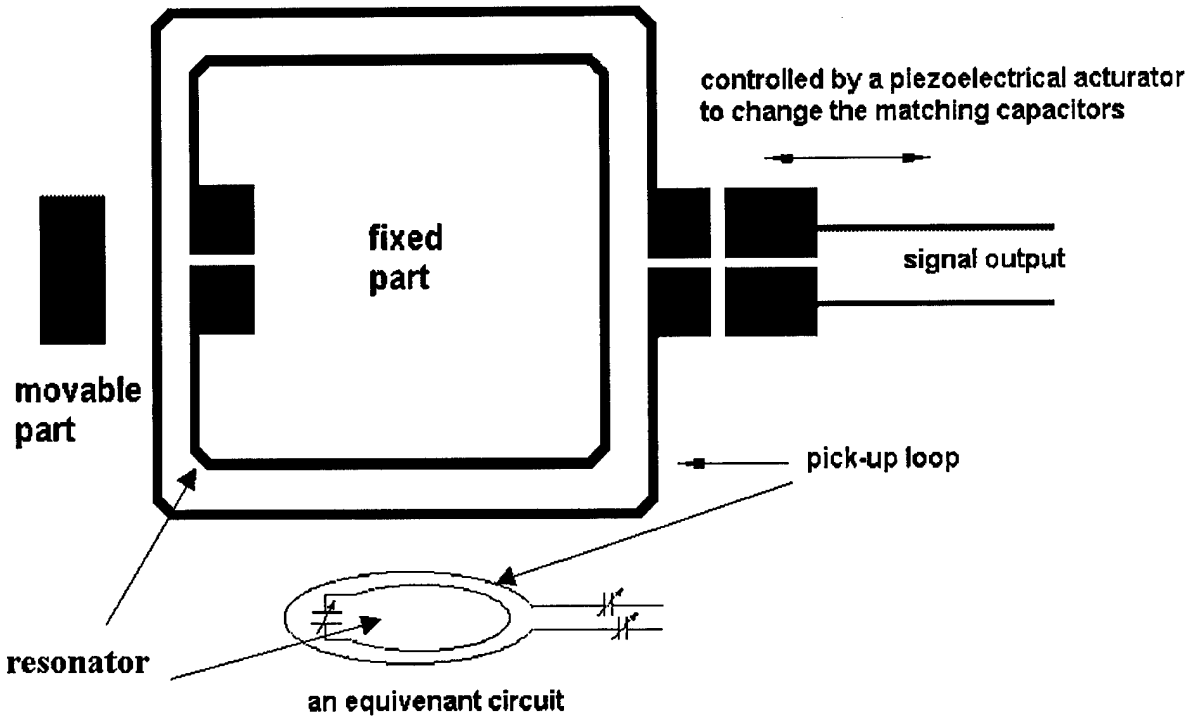

Fig. 26. Superconducting tunable capacitor used as matching capacitors

References

1. Erzhen Gao, Shapur Sahba, Hui Xu, Q.Y. Ma "A Superconducting RF Resonator in HF Range and its Multi-pole Filter Applications" IEEE Trans. App. Supercon. Vol 9, pp3066-69, June 1999.

2. Hui Xu, Erzhen Gao, et al. "Design and Implementation of A Lumped-Element Multipole HTS Filter at 15 MHz" IEEE Trans. App. Supercon. Vol 9, pp3886-88, June 1999.

3. Erzhen Gao, Shapur Sahba [+], Hui Xu, Q. Y. Ma, "High Temperature Superconducting Multi-pole RF Filter," submitted to IEEE-- Microwave Theory and Technology.

4. Hui Xu, E. Gao, et al. "A HTS Multipole Filter Operating at HF Range," American Physical Society, Centennial March Program, Atlanta, GA, 20-26 March 1999

5. Erzhen Gao, Shapur Sahba [+], Hui Xu, Q. Y. Ma, "A Superconducting RF Three-pole Filter in HF Range," 99 International Superconductive Electronics Conference, Claremont Resort, Berkeley, CA, June 21-25, 1999

6. Shapur Sahba, Erzhen Gao, Hui Xu, and Q.Y. Ma , "Superconducting Resonator and Filter Devices (P31976)," Patent Pending: Submitted on September 16, 1998

7. Shapur Sahba, Erzhen Gao, Hui Xu, and Q.Y. Ma , "High Temperature Superconducting Channelizing RF Filters," Patent Pending: Submitted on March 12, 1999

8. Frederick W. Grover, Inductance *Calculations Working Formulas and Tables* D.Van Nostrand Company, Inc. New York 1946.